Identification of Barkor as a mammalian autophagy-specific factor for Beclin 1 and class III phosphatidylinositol 3-kinase

Qiming Sun[a], Weiliang Fan[a], Keling Chen[a], Xiaojun Ding[b], She Chen[b], and Qing Zhong[a,1]

[a]Division of Biochemistry and Molecular Biology, Department of Molecular and Cell Biology, University of California, Berkeley, CA 94720; and [b]National Institute of Biological Sciences, Beijing 102206, China

Communicated by Xiaodong Wang, University of Texas Southwestern Medical Center, Dallas, TX, October 17, 2008 (received for review October 10, 2008)

Autophagy mediates the cellular response to nutrient deprivation, protein aggregation, and pathogen invasion in human. Dysfunction of autophagy has been implicated in multiple human diseases including cancer. The identification of novel autophagy factors in mammalian cells will provide critical mechanistic insights into how this complicated cellular pathway responds to a broad range of challenges. Here, we report the cloning of an autophagy-specific protein that we called Barkor (Beclin 1-associated autophagy-related key regulator) through direct interaction with Beclin 1 in the human phosphatidylinositol 3-kinase class III complex. Barkor shares 18% sequence identity and 32% sequence similarity with yeast Atg14. Elimination of Barkor expression by RNA interference compromises starvation- and rapamycin-induced LC3 lipidation and autophagosome formation. Overexpression of Barkor leads to autophagy activation and increased number and enlarged volume of autophagosomes. Tellingly, Barkor is also required for suppression of the autophagy-mediated intracellular survival of *Salmonella typhimurium* in mammalian cells. Mechanistically, Barkor competes with UV radiation resistance associated gene product (UVRAG) for interaction with Beclin 1, and the complex formation of Barkor and Beclin1 is required for their localizations to autophagosomes. Therefore, we define a regulatory signaling pathway mediated by Barkor that positively controls autophagy through Beclin 1 and represents a potential target for drug development in the treatment of human diseases implicated in autophagic dysfunction.

Atg14 | autophagosome | LC3 | *Salmonella* | UVRAG

One of the central regulators of autophagy in mammalian cells is Beclin 1 (1–3). Beclin 1 is a component of the class III phosphatidylinositol 3-kinase (PI3KC3) complex, which also contains a PI3K catalytic subunit and a regulatory subunit (p150) (4). *Beclin 1* was identified as a haploid insufficient tumor suppressor gene (3). It is monoallelically deleted in ovarian, breast, and prostate cancers. Heterozygous *Beclin* $1^{+/-}$ mice have reduced autophagy activity and increased incidence of spontaneous tumors (5, 6). Allelic loss of *Beclin 1* leads to genome instability upon metabolic stress (7, 8). All of this evidence illustrates a role for Beclin 1 and autophagy in cancer development.

Notably, Beclin 1 and PI3KC3 have pleiotropic functions in multiple cellular processes. PI3KC3 is not only required for autophagy, but also has broad functions in endocytic protein sorting (9). Functional equivalents of Beclin 1/PI3KC3/p150 in yeast, Vps30/Atg6-Vps15-Vps34, are known to play a critical role in autophagy and in vacuolar protein sorting (VPS) (1, 10). The specificity of PI3KC3 in yeast is determined by different complex compositions. Two regulatory proteins, Atg14 and Vps38, direct the core PI3K complex to either the phagophore assembly site (PAS) for autophagy or the endosome for VPS (10, 11), respectively, to execute their functions in autophagy or VPS. Atg14 is required for mediating the localization of the core PI3KC3 complex to PAS and is also important in recruiting downstream Atg proteins such as Atg2, Atg8, Atg16, and the Atg12-Atg5 conjugate to the PAS for membrane elongation and vesicle completion (12, 13). In contrast, Vps38 is responsible for the endosomal localization of the PI3K complex (11). Surprisingly, such regulatory mechanisms directing PI3KC3 specificity have not been identified in mammals.

How the function of Beclin 1 is specifically directed toward autophagosomes in mammalian cells has remained elusive. We speculate that there are autophagy-specific factors mediating Beclin 1 activity in autophagy. We used a biochemical approach to purify and proteomic methods to characterize the Beclin 1 complex. Here, we report the identification of a Beclin 1-associated protein that promotes autophagy specifically through the interaction with Beclin 1.

Results

Identification of Barkor as a Beclin 1-Interacting Protein. To search for Beclin 1 regulatory proteins, we generated a cell line from human osteosarcoma U_2OS cells that is stably transfected with ZZ-Beclin 1-FLAG under the control of doxycycline [supporting information (SI) Fig. S1*A*]. The expression of Beclin 1 was adjusted by the titration of doxycycline, and a dose (20 ng/mL) that induces expression of tagged Beclin 1 close to the endogenous level was selected (Fig. S1*B*). The tagged Beclin 1 was purified from cell extracts by sequential affinity chromatography steps, and the final FLAG peptide eluate was subjected to 4–12% gradient SDS/PAGE and visualized by silver staining (Fig. 1*A*). The indicated bands were excised and analyzed by mass spectrometry. In addition to the known components of the Beclin 1 complex, namely the PI3K catalytic subunit, p150 regulatory subunit, and UVRAG, we also identified a 68-kDa protein by mass spectrometry, KIAA0831 (Fig. 1*A*), which we called Barkor (Beclin 1-associated autophagy related key regulator). We were able to purify the same complex from human embryonic kidney 293T cells expressing tagged Beclin 1, indicating that the formation of this complex is not cell type-specific (Fig. 1*B*). Bioinformatic analysis revealed that Barkor contains an N-terminal zinc finger motif and a central coiled-coil domain (CCD) (Fig. S2) and a domain organization similar to Atg14 in yeast. Barkor also shares 18% sequence identity and 32% sequence similarity with yeast Atg14 (Fig. S3). The identities of these interacting proteins were further confirmed by immunoblotting analysis (Fig. S4). Although another Beclin 1-interacting protein, Bcl-2 (14), could not be visualized by silver staining, its presence in the final eluate was validated by immunoblotting (Fig. S4). The interaction of Barkor and Beclin 1 was further confirmed by the

Author contributions: Q.Z. designed research; Q.S., W.F., and K.C. performed research; X.D. and S.C. contributed new reagents/analytic tools; Q.S., W.F., and Q.Z. analyzed data; and Q.S. and Q.Z. wrote the paper.

The authors declare no conflict of interest.

Freely available online through the PNAS open access option.

[1]To whom correspondence should be addressed at: Department of Molecular and Cell Biology, University of California, 316 Barker Hall, Berkeley, CA 94720. E-mail: qingzhong@berkeley.edu.

This article contains supporting information online at www.pnas.org/cgi/content/full/0810452105/DCSupplemental.

© 2008 by The National Academy of Sciences of the USA

BIOCHEMISTRY

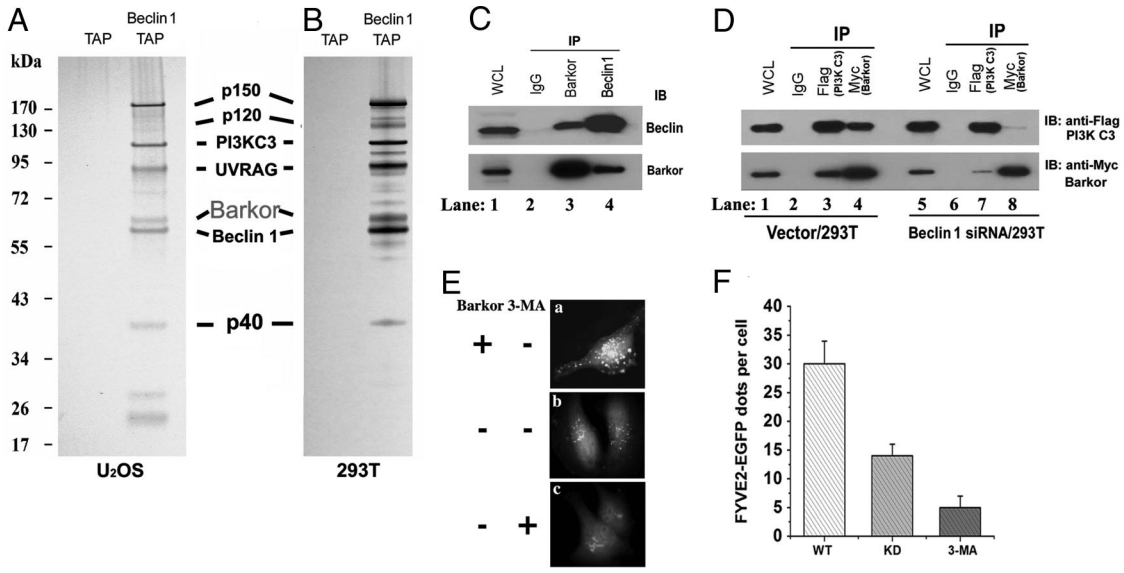

Fig. 1. Barkor is a major component of the Beclin 1–PI3KC3 complex. (*A*) Silver staining of the tandem affinity-purified Beclin 1 complex or vector alone in U_2OS cells. All the marked bands were identified by mass spectrometry. (*B*) A similar Beclin 1 complex was purified from human kidney embryonic HEK293T cells. (*C*) Reciprocal coimmunoprecipitation of Barkor and Beclin 1. 293T cell extracts were immunoprecipitated with either anti-Barkor or Beclin 1 antibody and then analyzed. (*D*) Beclin 1 bridges the interaction between PI3KC3 and Barkor. Beclin 1-knockdown 293T cells or control cells were transfected with FLAG-PI3KC3 and Myc-Barkor. Whole-cell lysates were immunoprecipitated with anti-FLAG or Myc antibodies and analyzed. (*E*) Barkor-knockdown decreases the activity of PI3KC3 in vivo. Barkor-knockdown U_2OS cells were transfected with FYVE2-EGFP expression vector. Thirty hours after transfection, cells were treated with 5 mM 3-MA for another 4 h. FYVE2-EGFP was quantified in *F*.

reciprocal endogenous coimmunoprecipitation of Barkor and Beclin 1 with each other's antibodies (Fig. 1*C*).

Barkor Is Important for Efficient Production of PI3P in Vivo. Because Beclin 1 is a major component of the PI3KC3 complex, we checked whether Barkor is also a component of this complex. Indeed, Barkor and Beclin 1 were coimmunoprecipitated with PI3KC3 antibody (Fig. S5), indicating that Barkor is part of the PI3KC3 complex.

The interaction between Beclin 1 and PI3KC3 was not affected by either Barkor-knockdown (Fig. S6 *A* and *B*) or overexpression (Fig. S6*C*). Because Barkor interacts directly with Beclin 1, we asked whether Beclin 1 is required for the association between PI3KC3 and Barkor. Indeed, in Beclin 1-knockdown (Fig. S6*D*) cells, the amount of Barkor in the PI3KC3 immunoprecipitate (Fig. 1*D*, lane 7) was dramatically reduced compared with that in Beclin 1-proficient cells (Fig. 1*D*, lane 3). The amount of PI3KC3 in Barkor immunoprecipitate in Beclin 1-knockdown cells (Fig. 1*D*, lane 8) was also greatly compromised compared with that in Beclin 1-proficient cells (Fig. 1*D*, lane 4). In summary, Beclin 1 is required for the interaction between PI3KC3 and Barkor.

To test whether Barkor might regulate PI3KC3 activity, we measured its lipid phosphorylation activity in wild-type and Barkor-knockdown cells. PI3KC3 phosphorylates the 3′-hydroxyl position of the phosphatidylinositol (PtdIns) ring to produce PtdIns3*P* (PI3P) (9). The production of PI3P by PI3KC3 could be visualized and quantified by fluorescence of the GFP-tagged double FYVE finger of the Hrs protein (15). Because the FYVE probe specifically binds to PI3P, the only end product of PI3KC3, we could measure PI3KC3 activity by detecting FYVE fluorescence. PI3P production was diminished in Barkor knockdown cells compared to that in wild-type cells, and could be further depleted by treatment of the PI3K inhibitor 3-methyladeline (3-MA) (Fig. 1 *E* and *F*).

Barkor Is Required for LC3 Conjugation and Autophagosome Assembly. To demonstrate the role of Barkor in autophagy directly, we generated doxycycline-inducible RNAi-knockdown cell lines for both Beclin 1 and Barkor in U_2OS cells (Fig. S7 *A* and *B*). A faithful marker of autophagy activity is LC3 conjugation to phosphatidylethanolamine (PE), which is strongly induced by stimuli such as starvation or rapamycin treatment (16). The LC3-conjugated form (also called LC3II) migrates slightly faster than the cytosolic free form (LC3I). In wild-type cells, the LC3II form was dramatically increased upon starvation (Fig. 2*A*, lanes 3 and 7) compared with that in untreated cells (Fig. 2*A*, lanes 1 and 5). However, in Barkor-inducible knockdown cells, the LC3II form was decreased (Fig. 2*A*, lane 8) at a level comparable with that of Beclin 1-knockdown cells (Fig. 2*A*, lane 4). Similarly, LC3II was strongly induced in rapamycin-treated wild-type cells (Fig. 2*B*, lane 3), but not in the Barkor-knockdown cells (Fig. 2*B*, lane 7). Pretreatment with the protease inhibitors pepstatin and E-64D accumulated the LC3II form in rapamycin-treated (Fig. 2*B*, lane 4) and untreated (Fig. 2*B*, lane 2) Barkor-proficient cells, but had no effect on LC3 conjugation in Barkor-deficient cells (Fig. 2*B*, lanes 6 and 8). All of these data indicate that Barkor is essential for LC3 conjugation to PE and for autophagy activation. Consistently, LC3 puncta were also dramatically compromised in Barkor knockdown cells (Fig. S8).

To visualize autophagosome formation directly, we performed an electron microscopic analysis. During autophagy, cytoplasmic components, including proteins and organelles, are engulfed by double-membrane autophagosomes, which fuse to lysosomal vesicles to form autolysosomes where the contents are degraded into their components (17). Autophagic vacuoles (AVs) that include autophagosomes and autolysosomes could be captured under transmission electron microscope and are shown as double-membrane vesicles (autophagosomes) or single-membrane vesicles (autolysosomes) that contain intracellular contents including cytosol and organelles (mitochondria and/or endoplasmic reticulum) (Fig. 2*E*, marked by arrows) (17). In Barkor wild-type cells, we observed abundant AVs in response to nutrient deprivation (Fig. 2 *C*, *E*, and *F*). AVs were rarely observed in Barkor-knockdown cells (Fig. 2 *D* and *F*).

We then asked whether forced expression of Barkor would stimulate autophagosome formation. For this purpose, we set up a Barkor stable overexpression (OE) cell line in U_2OS, and

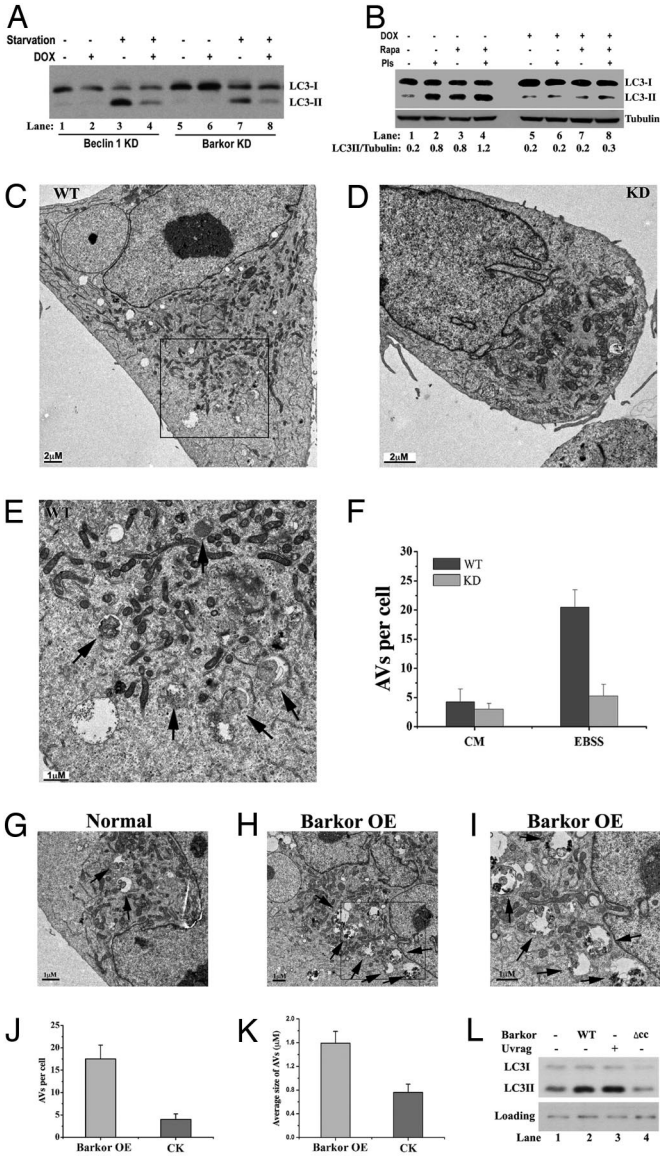

Fig. 2. Barkor is required for LC3 lipidation and autophagosome formation. (*A*) LC3 conjugation was examined in Beclin 1 and Barkor-knockdown U_2OS cells in complete medium (DMEM + 10% FBS) or starvation medium (Earle's balanced salt solution, EBSS). (*B*) LC3 conjugation was examined in Barkor-knockdown cells treated with 500 nM rapamycin overnight. Proteases inhibitors (2 μg/mL E64D and 2 μg/mL pepstatin for 4 h) were used to block lysosomal degradation. (*C–E*). Electron microscopic (EM) analysis of Barkor-knockdown cells. Both control cells (*C*) and Barkor-knockdown cells (*D*) were starved in EBSS for 1 h and analyzed by transmission electron microscopy. (*E*) High-magnification picture of the framed area in *C* showing AVs (marked by arrows) that contain intracellular contents. [Scale bars: 2 μM (*C*), 2 μM (*D*), and 1 μM (*E*).] (*F*) AVs per cross-sectioned cell (mean $\pm$ SD; $n = 21$) under EM were calculated and summarized. CM, complete medium. Arrows indicate autophagic vacuole. (*G–I*) Barkor-overexpression (OE) U_2OS cells (*H* and *I*) and U_2OS parental cells (*G*) were observed under EM. (*I*) High-magnification picture of the framed area in *H* shows AVs (marked by arrows) that contain intracellular contents. [Scale bars: 1 μM (*G–I*).] (*J*) AVs per cross-sectioned cell under EM were calculated. (*K*) The average size of AVs in Barkor OE cells or normal cells was calculated and summarized. (*L*) HEK293T cells were transfected with Barkor (wild-type or CCD deletion mutant) or UVRAG, and LC3 conjugation was examined in these cells.

autophagic vacuole formation was observed in these cells. The number of AVs was dramatically increased in Barkor OE cells (Fig. 2 *H*–J) compared with that in parental cells (Fig. 2 *G* and *J*). Also, AVs in Barkor OE cells were more heterogeneous, and we observed a significant amount of large AVs (Fig. 2 *H* and *I*). The average size of AVs in Barkor OE cells was nearly doubled compared with that in control cells (Fig. 2*K*). Consistently, overexpression of Barkor in HEK293T cells led to autophagy activation, illustrated by increasing amounts of the LC3II form (Fig. 2*L*). All of these data demonstrate that Barkor is important in autophagosome formation and expansion.

Barkor Is Critical for Autophagy-Mediated Bacterial Clearance. Autophagy has been recognized as an important defensive mechanism to suppress bacterial infection (18). It has been reported that infection by *Salmonella typhimurium*, a causative agent for food poisoning and typhoid fever, is controlled by autophagy (19–21). We first asked whether autophagy is required for controlling bacterial infection in nonphagocytic mammalian cells. Mouse embryonic fibroblasts (MEFs) knocked out of *Atg7* (22), an essential gene for autophagy, were infected with *Salmonella* marked with GFP, and uptake of *Salmonella* was monitored microscopically by green fluorescence. As expected, $Atg7^{-/-}$ MEFs were more permissive for intracellular replication by *Salmonella* than wild-type cells, allowing remarkably increased GFP fluorescence in the cytosol (Fig. 3*A*). We further performed a quantitative assay to measure the bacterial growth. *Salmonella* growth was accelerated in *Atg7*-knockout cells compared with wild-type cells (Fig. 3*B*), confirming that autophagy is required for *Salmonella* amplification in nonphagocytic mammalian cells.

A similar phenomenon was observed in Barkor-knockdown cells, namely that there was more bacterial growth when Barkor protein was eliminated (Fig. 3*C*). The same quantitative assay for bacterial growth indicated that a 2- to 3-fold increase in bacterial replication could be detected in Barkor-deficient over Barkor-proficient cells (Fig. 3*D*). This result demonstrates that Barkor is crucial for autophagy-mediated bacterial elimination in mammalian cells.

Barkor Interacts with Beclin 1 Through CCDs. We performed an in-depth analysis of the interaction between Barkor and Beclin 1. We constructed a series of vectors that express various deletion mutants of both Beclin 1 and Barkor on the basis of their putative structures. Barkor contains an N-terminal zinc finger motif and a central CCD (Fig. 4*A*), and Beclin 1 consists of 3 domains: an N-terminal BH3 domain, a central CCD, and an evolutionarily conserved domain at the C terminus (Fig. 4*B*) (23). IP assays showed that all of the Barkor fragments containing CCD, including CCD alone (Fig. 4*A*, lanes 2, 4, 5, and 6), immunoprecipitated Beclin 1, whereas Barkor fragments lacking CCD failed to bind (Fig. 4*A*, lanes 3 and 7), demonstrating that Barkor specifically binds to Beclin 1 through its CCD (Fig. 4*A*). Additionally, Beclin 1 specifically interacts with Barkor through its CCD as well (Fig. 4*B*).

Barkor and UVRAG Form Mutually Exclusive Complexes with Beclin 1. UVRAG is a recently identified positive regulator of Beclin 1 (24) and interacts with Beclin 1 through a CCD interaction. Because the same binding surface of Beclin 1 is used to bind to both Barkor and UVRAG, we speculated that Barkor and UVRAG might form mutually exclusive complexes with Beclin 1 through competition. To test this hypothesis, we examined the direct interaction among Barkor, UVRAG, and Beclin 1 in an in vitro binding assay. In this assay, we purified different recombinant CCDs of Beclin 1, Barkor, and UVRAG from *Escherichia coli* (Fig. S9) and performed in vitro binding reactions. As shown in Fig. 4*C* (*Bottom*), both Barkor CCD (lane 4) and UVRAG CCD (lane 6) bound to Beclin 1 CCD directly. Similar experiments were performed by using Barkor CCD (Fig. S10*A*) or UVRAG CCD (Fig. S10*B*) as baits; both CCDs bind to Beclin 1 but not to each other.

We further investigated whether Barkor and UVRAG form

BIOCHEMISTRY

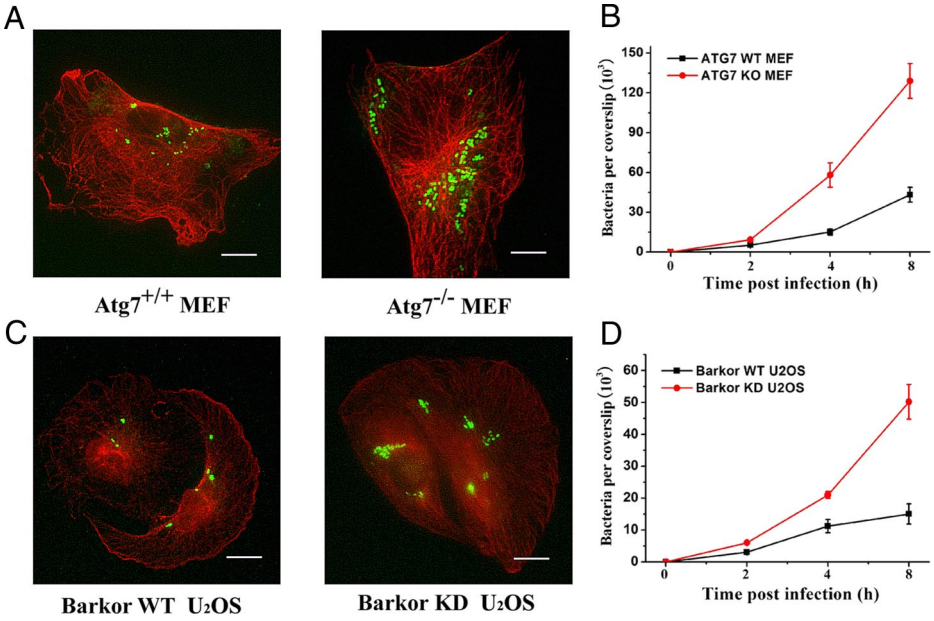

Fig. 3. Barkor is indispensable for autophagy-mediated suppression of bacterial replication in vivo. (*A*) *Atg7*$^{+/+}$ *and Atg7*$^{-/-}$ MEFs cells were infected with wild-type GFP-marked *S. typhimurium* (SL1344) (green) for 8 h and analyzed by immunostaining. Cells were counterstained with anti-tubulin antibody (red). (*B*) *Atg7*$^{+/+}$ or *Atg7*$^{-/-}$ MEFs were infected with *S. typhimurium* (SL1344) for indicated times. The infected cells were treated with gentamicin sulfate to block extracellular bacterial amplification and then lysed, and internalized bacteria were plated on Petri dishes. The replication of bacteria was quantified by counting the colony number on the Petri plates. (*C*) Barkor-knockdown U_2OS cells were induced by doxycycline for 2 days and infected with *S. typhimurium* as described in *A*. (*D*) The bacterial growth in Barkor-knockdown U_2OS cells was measured as described in *B*.

mutually exclusive subcomplexes with Beclin 1 in vivo. We performed coimmunoprecipitation experiments to detect Beclin 1, Barkor, and UVRAG interactions in vivo. Beclin 1 antibody (Fig. 4*D*, lane 3) but not control antibody (Fig. 4*D*, lane 2) immunoprecipitated with both Barkor and UVRAG. However, Beclin 1 interacted with both Barkor and UVRAG,

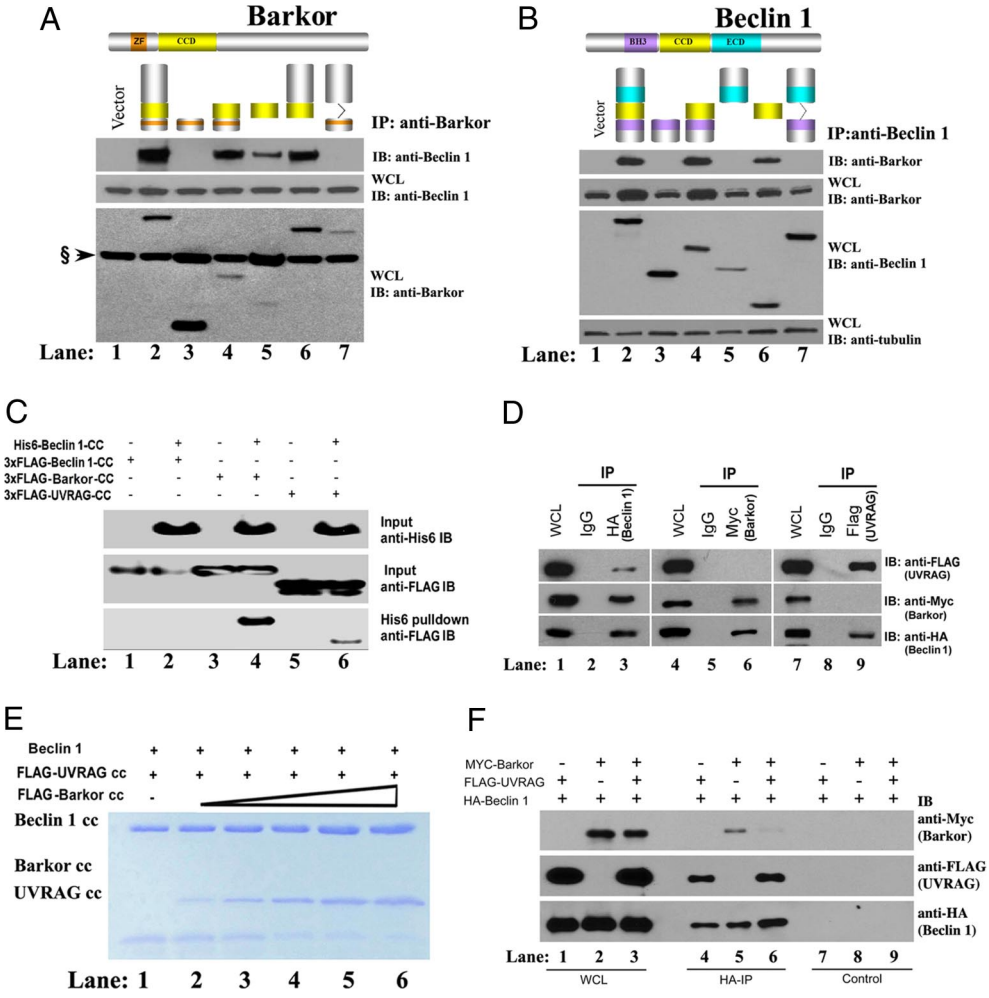

Fig. 4. Barkor and UVRAG form distinct subcomplexes with Beclin 1 through their CCDs. (*A*) Barkor binds to Beclin 1 through its CCD. 293T cells were transfected with FLAG-Beclin 1, Myc-Barkor, or its Myc-tagged mutants. Whole-cell lysates (WCLs) were immunoprecipitated (IP) with anti-Myc followed by immunoblotting (IB) with anti-FLAG. § indicates a nonspecific band. (*B*) Beclin 1 binds to Barkor through its CCD. 293T cells were transfected with Myc-Barkor, FLAG-Beclin 1, or its FLAG-tagged mutants. WCLs were immunoprecipitated with anti-FLAG followed by the IB with anti-Myc. (*C*) Direct interaction of Beclin 1 with Barkor or UVRAG. A Ni-column was incubated first with His-Beclin 1-CC and then with FLAG-tagged Beclin 1-CC, Barkor-CC, and UVRAG-CC. Proteins bound to beads and inputs were analyzed. (*D*) Barkor and UVRAG form distinct subcomplexes with Beclin 1. 293T cells were transfected with FLAG-UVRAG, Myc-Barkor, and HA-Beclin 1. WCLs were immunoprecipitated with anti-FLAG, anti-HA, or Myc, and the immunoprecipitates were analyzed. (*E*) Barkor competes with UVRAG for binding to Beclin 1. UVRAG was first incubated with Beclin 1 in vitro; increasing doses of the Barkor CCD were then added to the reactions. After extensive washing, the proteins bound to beads were analyzed by SDS/PAGE stained with Coomassie blue. (*F*) UVRAG competes with Barkor–Beclin 1 interaction in vivo. HA-Beclin 1 was cotransfected into HEK293T cells with Myc-Barkor or FLAG-tagged UVRAG. WCLs were immunoprecipitated with anti-HA followed by the IB with antibodies against Myc, FLAG, or HA.

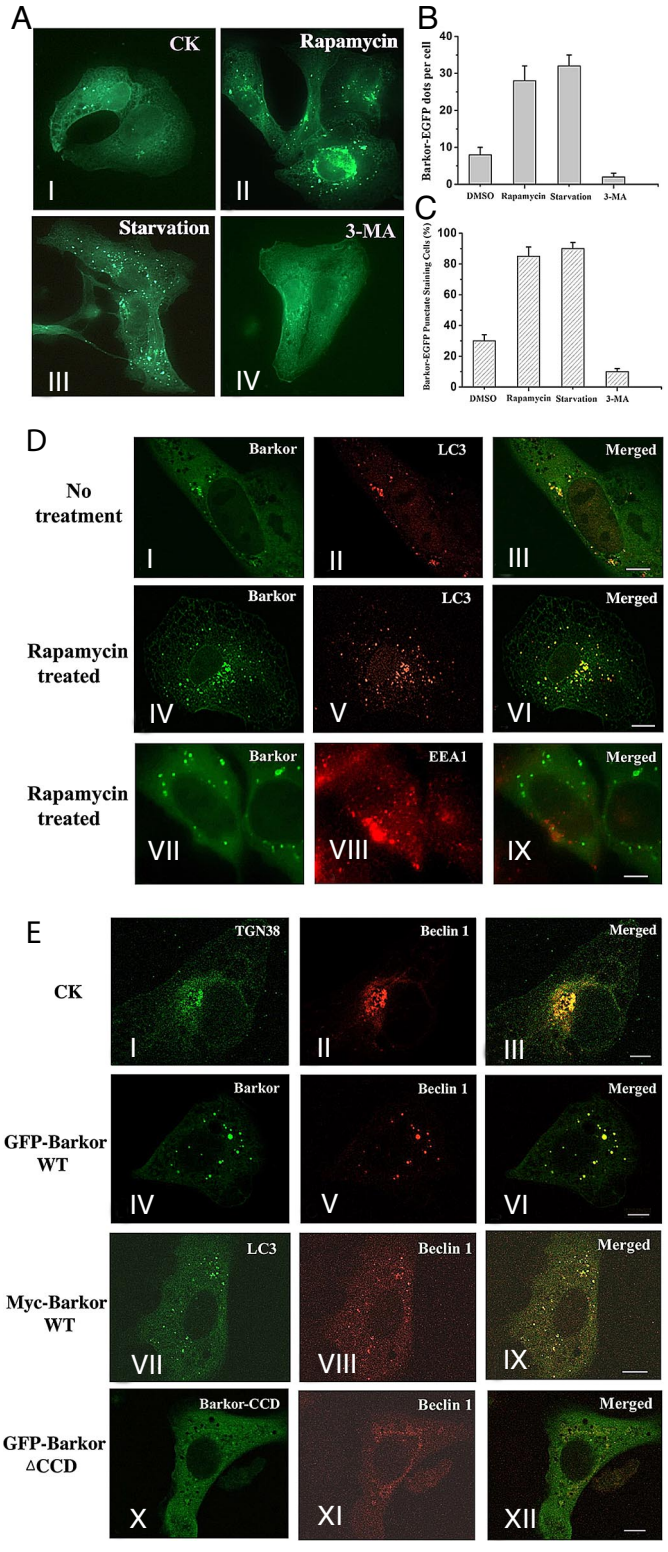

Fig. 5. Barkor promotes Beclin 1 translocation to autophagosomes through direct interaction. (*A*) Subcellular localization of Barkor. Fluorescent Barkor-EGFP detected in transfected U_2OS cells upon mock treatment (*I*), 500 nM rapamycin (*II*), EBSS medium (*III*), or EBSS and 5 mM 3-MA, respectively, under a fluorescence microscopy. (*B*) Quantification of Barkor-EGFP dots per cell. (*C*) Quantification of Barkor-EGFP punctate staining-positive cells. (*D*) Colocalization of Barkor and LC3. A U_2OS stable cell line expressing Myc-LC3 was transfected with Barkor-EGFP and then mock treated (*I–III*) or treated with 500 nM rapamycin (*IV–IX*) for 12 h. (*I–VI*) GFP-Barkor (green) was costained with Myc-LC3 (red). (*VII–IX*) GFP-Barkor (green) was costained with endogenous EEA1 (red) (an endosome marker). (*E*) U_2OS cells were transfected with RFP-Beclin 1. (*I–III*) RFP-Beclin 1 was costained with endogenous TGN38 (green) (a *trans*-Golgi network marker). (*IV–VI*) U_2OS cells were transfected with Barkor-EGFP (green) and RFP-Beclin 1 (red), and fluorescence of Barkor-EGFP (green) and RFP-Beclin 1 (red) was observed. (*VII–IX*) U_2OS cells were transfected with RFP-Beclin 1, Myc-Barkor, and GFP-LC3, and fluorescence of GFP-LC3 (green) and RFP-Beclin 1 (red) was observed. (*X–XII*), U_2OS cells were transfected with RFP-Beclin 1 and Barkor CCD-deletion mutant-fused EGFP, and the fluorescence of GFP-Barkor CCD deletion (green) and RFP-Beclin 1 (red) was observed.

but no interaction was detected between Barkor and UVRAG (Fig. 4*D*).

We then asked whether Barkor competes with UVRAG for Beclin 1 binding. In the binding assay, we first incubated His_6-Beclin 1 CCD with Ni-beads and then with UVRAG CCD to allow Beclin 1–UVRAG (Fig. 4*E*) complex formation. Excess amounts of Barkor CCD were added to the reaction mixture at different concentrations to compete with UVRAG–Beclin 1 binding. As expected, UVRAG CCD was displaced from the Beclin 1 complex in a dose-dependent manner (Fig. 4*E*). A similar competition assay was performed in vivo by coimmunoprecipitation. Barkor could be efficiently coimmunoprecipitated with antibodies against HA-Beclin 1 (Fig. 4*F*, lane 5). However, Beclin 1–Barkor interaction was diminished when UVRAG was overexpressed (Fig. 4*F*, lane 6). Therefore, an excess amount of UVRAG could compete with the Beclin 1–Barkor interaction in vivo. These results indicate that Barkor and UVRAG interact with Beclin 1 in a mutually exclusive manner through direct competition.

Subcellular Localization of Barkor Is Regulated by Autophagy Stress. We first investigated Barkor subcellular localization in human osteosarcoma U_2OS cells transfected with GFP-Barkor. Approximately 20% of GFP-positive cells displayed a scarce punctate staining, and the rest showed a diffuse cytoplasmic staining (Fig. 5*AI*). The percentage of cells containing abundant Barkor foci was dramatically augmented (≈80%) by treatment with the autophagy inducer rapamycin (Fig. 5*AII*) or nutrient withdrawal (Fig. 5*AIII*). Treatment with the autophagy inhibitor 3-MA converted the punctate pattern of Barkor to a diffuse cytoplasmic staining (Fig. 5*AIV*). A statistical analysis of foci per cell or number of cells with foci was also consistent with the observations (Fig. 5 *B* and *C*). The Barkor punctate staining colocalized nearly perfectly with LC3 in the unstressed condition (Fig. 5*D I–III*) or upon rapamycin treatment (Fig. 5*D IV–VI*). All of these results prove that Barkor resides predominantly on autophagosomes, which is regulated by autophagy stimuli. As a control, there was no apparent overlap between Barkor and the early endosome marker EEA1 before or after rapamycin treatment (Fig. 5*D VII–IX* and data not shown).

Barkor Promotes Beclin 1 Translocation to Autophagosomes. We next asked whether Barkor would affect Beclin 1 distribution through direct interaction. In yeast, Atg6 localizes to the PAS, and this localization is required for the recruitment of downstream autophagy proteins (11, 12). However, in mammalian cells, Beclin 1 normally localizes to the *trans*-Golgi network (4) (Fig. 5*E I–III*). It is still elusive how Beclin 1 participates in autophagosome assembly. Given the location of Barkor on autophagosomes (Fig. 5*D*), we speculate that Barkor might promote the translocation of Beclin 1 from the *trans*-Golgi network to autophagosomes.

We examined the localization of Beclin 1 in the presence of Barkor expression. When Barkor (GFP-tagged) and Beclin 1 (RFP-tagged) were coexpressed, nearly all Barkor and Beclin 1 proteins were colocalized in cytoplasmic foci (Fig. 5*E IV–VI*). These Barkor/Beclin 1-decorated foci overlapped perfectly with the LC3 staining (Fig. 5*E VII–IX*), indicating that Beclin 1 is localized to the autophagosome. The distribution of Barkor and Beclin 1 on autophagosomes is mediated by their interaction because a Barkor

BIOCHEMISTRY

mutant lacking its CCD failed to localize to autophagosomes and failed to direct Beclin 1 to autophagosomes (Fig. 5*E X–XII*). Therefore, complex formation of Barkor and Beclin 1 is required for their localization to autophagosomes.

Discussion

Barkor Promotes Autophagy Through Interaction with Beclin 1. In this work, we reported the purification of the Beclin 1 complex from human cells. In addition to its core components of Beclin 1, PI3KC3 and p150, and a known autophagy regulatory protein UVRAG, a unique protein Barkor has also been identified in this complex. Barkor interacts with Beclin 1 directly through its central CCD in a way similar to the Beclin 1–UVRAG interaction. Consequently, Barkor and UVRAG compete with each other for their interaction with Beclin 1 and actually form distinct complexes in mammalian cells. Barkor seems to be critical for mammalian autophagy because knockdown of this protein from mammalian cells compromises their ability to activate autophagy in response to nutrient deprivation and bacterial infection. Overexpression of Barkor leads to autophagy activation and augmentation of autophagosome formation. Finally, the Barkor–Beclin 1 interaction is required for their localization to autophagosomes.

Barkor Could Be the Mammalian Functional Ortholog of Atg14 in Yeast. Based on the sequence alignment and functional similarity, Barkor is a good candidate to be the mammalian functional ortholog of Atg14, the autophagy-specific regulatory factor for Atg6/Beclin 1 in yeast (10, 11). Both Barkor and Atg14 possess a zinc finger motif at the N terminus and a central CCD. Barkor also shares 18% sequence identity and 32% sequence similarity with yeast Atg14 (Fig. S3). Critically, both Barkor and Atg14 direct Beclin 1/Atg6 to the autophagosome.

It is interesting to note that Barkor competes with UVRAG for its binding to Beclin 1, similar to the interplay between Atg14 and Vps38 in yeast. Coincidentally, a recent study suggests that UVRAG is involved in late endosome fusion with the lysosome, a phenomenon equivalent to vacuolar protein sorting in yeast, through its interaction with the HOPS/Vps C complex (25). It is possible that Barkor and UVRAG mediate the activity of Beclin 1 in autophagy and vacuole protein sorting, respectively. However, evidence for the UVRAG role in autophagy (24) also demands an alternative model. In this model, Barkor and UVRAG may interact with Beclin 1 in a stepwise manner and mediate its function in early autophagosome formation and late autophagosome/lysosome fusion sequentially.

How the autophagosome is formed is still an open question in this field. The identification of Barkor and 2 other factors in the Beclin 1 complex will provide an opportunity perhaps to allow in vitro reconstitution of PI3K function and autophagosome formation.

Materials and Methods

The full-length cDNAs of human Barkor (KIAA0831), Beclin 1, UVRAG, and PI3KC3 were purchased from Open Biosystem. The shRNA coding sequence for Barkor knockdown is GATCCCC**GAAGGAAAGGTTAAGCCGA**TTCAAGAGATCGGCTTAACCTTTCCTTCTTTTTA. The rest of the information about reagents, cell lines, cell lysates preparation, tandem affinity purification, coimmunoprecipitation, immunostaining, electronic microscopy, autophagy analysis, and bacterial infection is listed in *SI Experimental Procedures*.

ACKNOWLEDGMENTS. We thank all of the Zhong laboratory members for helpful discussion and technical assistance; Terje Johansen (University of Tromso), Jae Jung (University of Southern California), Harald Stenmark (Univeristy of Oslo), Masaaki Komatsu (Juntendo University School of Medicine), and Denise Monack (Stanford University School of Medicine) for reagents; Xiaodong Wang, Robert Tjian, Randy Schekman, Daniel Klionsky, Jeremy Thorner, and Yulia Mostovoy for critical reading of the manuscript; Nick V. Grishin at the University of Texas Southwestern Medical Center for a bioinformatic analysis of Barkor; Dr. Yumay Chen at the University of Texas Health Science Center at San Antonio and Abmart at Shanghai for Barkor and Beclin 1 antibody production. The work was supported in part by a New Investigator Award for Aging from the Ellison Medical Foundation (to Q.Z.).

1. Cao Y, Klionsky DJ (2007) Physiological functions of Atg6/Beclin 1: A unique autophagy-related protein. *Cell Res* 17:839–849.
2. Levine B (2005) Eating oneself and uninvited guests: Autophagy-related pathways in cellular defense. *Cell* 120:159–162.
3. Liang XH, *et al.* (1999) Induction of autophagy and inhibition of tumorigenesis by Beclin 1. *Nature* 402:672–676.
4. Kihara A, Kabeya Y, Ohsumi Y, Yoshimori T (2001) Beclin–phosphatidylinositol 3-kinase complex functions at the *trans*-Golgi network. *EMBO Rep* 2:330–335.
5. Qu X, *et al.* (2003) Promotion of tumorigenesis by heterozygous disruption of the Beclin 1 autophagy gene. *J Clin Invest* 112:1809–1820.
6. Yue Z, Jin S, Yang C, Levine AJ, Heintz N (2003) Beclin 1, an autophagy gene essential for early embryonic development, is a haploinsufficient tumor suppressor. *Proc Natl Acad Sci USA* 100:15077–15082.
7. Karantza-Wadsworth V, *et al.* (2007) Autophagy mitigates metabolic stress and genome damage in mammary tumorigenesis. *Genes Dev* 21:1621–1635.
8. Mathew R, *et al.* (2007) Autophagy suppresses tumor progression by limiting chromosomal instability. *Genes Dev* 21:1367–1381.
9. Backer JM (2008) The regulation and function of class III PI3Ks: Novel roles for Vps34. *Biochem J* 410:1–17.
10. Kihara A, Noda T, Ishihara N, Ohsumi Y (2001) Two distinct Vps34 phosphatidylinositol 3-kinase complexes function in autophagy and carboxypeptidase Y sorting in *Saccharomyces cerevisiae*. *J Cell Biol* 152:519–530.
11. Obara K, Sekito T, Ohsumi Y (2006) Assortment of phosphatidylinositol 3-kinase complexes: Atg14p directs association of complex I to the preautophagosomal structure in *Saccharomyces cerevisiae*. *Mol Biol Cell* 17:1527–1539.
12. Suzuki K, Kubota Y, Sekito T, Ohsumi Y (2007) Hierarchy of Atg proteins in preautophagosomal structure organization. *Genes Cells* 12:209–218.
13. Suzuki K, *et al.* (2001) The preautophagosomal structure organized by concerted functions of APG genes is essential for autophagosome formation. *EMBO J* 20:5971–5981.
14. Pattingre S, *et al.* (2005) Bcl-2 antiapoptotic proteins inhibit Beclin 1-dependent autophagy. *Cell* 122:927–939.
15. Gillooly DJ, *et al.* (2000) Localization of phosphatidylinositol 3-phosphate in yeast and mammalian cells. *EMBO J* 19:4577–4588.
16. Klionsky DJ, Cuervo AM, Seglen PO (2007) Methods for monitoring autophagy from yeast to human. *Autophagy* 3:181–206.
17. Klionsky DJ, *et al.* (2008) Guidelines for the use and interpretation of assays for monitoring autophagy in higher eukaryotes. *Autophagy* 4:151–175.
18. Levine B, Deretic V (2007) Unveiling the roles of autophagy in innate and adaptive immunity. *Nat Rev* 7:767–777.
19. Hernandez LD, Pypaert M, Flavell RA, Galan JE (2003) A *Salmonella* protein causes macrophage cell death by inducing autophagy. *J Cell Biol* 163:1123–1131.
20. Birmingham CL, Smith AC, Bakowski MA, Yoshimori T, Brumell JH (2006) Autophagy controls *Salmonella* infection in response to damage to the *Salmonella*-containing vacuole. *J Biol Chem* 281:11374–11383.
21. Rioux JD, *et al.* (2007) Genome-wide association study identifies new susceptibility loci for Crohn disease and implicates autophagy in disease pathogenesis. *Nat Genet* 39:596–604.
22. Komatsu M, *et al.* (2006) Loss of autophagy in the central nervous system causes neurodegeneration in mice. *Nature* 441:880–884.
23. Furuya N, Yu J, Byfield M, Pattingre S, Levine B (2005) The evolutionarily conserved domain of Beclin 1 is required for Vps34 binding, autophagy, and tumor suppressor function. *Autophagy* 1:46–52.
24. Liang C, *et al.* (2006) Autophagic and tumour suppressor activity of a novel Beclin 1-binding protein UVRAG. *Nat Cell Biol* 8:688–699.
25. Liang C, *et al.* (2008) Beclin 1-binding UVRAG targets the class C Vps complex to coordinate autophagosome maturation and endocytic trafficking. *Nat Cell Biol* 10:776–787.